

Native defects in silver orthophosphate and their effects on photocatalytic activity under visible light irradiation

by Admin Publikasi

Submission date: 25-Jun-2022 04:14PM (UTC+0700)

Submission ID: 1862662319

File name: APSUS-Native_defects.pdf (539.59K)

Word count: 4907

Character count: 25039



Contents lists available at ScienceDirect

Applied Surface Science

journal homepage: www.elsevier.com/locate/apsusc



Full Length Article

Native defects in silver orthophosphate and their effects on photocatalytic activity under visible light irradiation



Uyi Sulaeman^{a,*}, Dadan Hermawan^a, Roy Andreas^a, Ahmad Zuhairi Abdullah^b, Shu Yin^c

^a Department of Chemistry, Jenderal Soedirman University, Purwokerto, 53123, Indonesia

^b School of Chemical Engineering, Universiti Sains Malaysia, 14300, Nibong Tebal, Penang, Malaysia

^c Institute of Multidisciplinary Research for Advanced Materials, Tohoku University, Sendai, 980-8577, Japan

ARTICLE INFO

Article history:

Received 21 May 2017

Received in revised form 9 September 2017

Accepted 22 September 2017

Available online 28 September 2017

Keywords:

Defect

Co-precipitation

Photocatalyst

Silver orthophosphate

Silver vacancy

ABSTRACT

Native defects in silver orthophosphate could be generated by simple co-precipitation method under ethanol-aqueous solution using AgNO_3 and $\text{Na}_2\text{HPO}_4 \cdot 12\text{H}_2\text{O}$. AgNO_3 ethanol-aqueous solution with the ethanol contents of 0%, 25%, 50%, 75%, 90% and 100% was reacted with Na_2HPO_4 aqueous solution. The produced catalysts were characterized using XRD, DRS, FE-SEM, BET specific surface area and XPS. The increase of ethanol content in the synthesis process decreased the Ag/P atomic ratio of Ag_3PO_4 . The native defects of silver vacancy might be generated on the surface of Ag_3PO_4 . The activity of Ag_3PO_4 for Rhodamine B degradation dramatically increased by 5.8 times higher compared to that of the pristine Ag_3PO_4 . The defect states of Ag vacancies enhanced the separation of electron-hole pairs, leading to the improvement of photocatalytic activity.

© 2017 Elsevier B.V. All rights reserved.

1. Introduction

The improvement of Ag_3PO_4 activity for organic pollutant degradation has been mostly achieved by three strategies. The first is the design of particular morphology to generate high reactivity on the surface of Ag_3PO_4 . These could create high surface energy [1] and the desired facet formation [2–4] to boost the activity of Ag_3PO_4 photocatalyst. The tetrahedron [1,4,5], tetrapod [3,6], ellipsoid [7] generally showed high activity under visible light irradiation. The high activity of tetrahedral Ag_3PO_4 is caused by {111} facets that contain only Ag atom [5]. The enriched Ag^+ cation in the {111} plane of Ag_3PO_4 could be partly reduced by photogenerated electron forming Ag nanolayers. These layers can facilitate the separation of photoexcited electron-hole pairs. The partially reduced Ag^+ site might produce a neighboring oxygen vacancy that increased the number of photocatalytic active sites. The tetrahedral morphology could also suppress the recombination of electron-hole pairs [4]. Saddle-like morphology of Ag_3PO_4 derived from tetrahedron also shows high photocatalytic activity due to an enriched Ag^+ on the surface [8]. The improved activity of tetrapod Ag_3PO_4 under visible light might be caused by the high activity of {110} facets [3,6] whereas the enhanced activity of the ellipsoid Ag_3PO_4 is caused by

the clean surface of this particle and smaller band gap energy [7]. Morphology-dependent photocatalytic properties are very promising to provide the way forwards for highly active photocatalysts.

The second strategy of improving the Ag_3PO_4 activity is the design of heterostructure materials. These materials could prevent Ag_3PO_4 photocorrosion during the photocatalytic reaction and can enhance the separation of photogenerated electron and holes. The photocorrosion reaction always occurs in Ag_3PO_4 as its conduction band (CB) potential is more positive than the hydrogen potential which limits its potential applications in photocatalysis. Therefore many researchers have been dealing with this issue. The heterostructures of $\text{Ag}_3\text{PO}_4/\text{TiO}_2$ [9–12], $\text{Ag}_3\text{PO}_4/\text{Cr-SrTiO}_3$ [13], $\text{Co}_3\text{O}_4/\text{Ag}_3\text{PO}_4$ [14], $\text{Ag}_3\text{PO}_4/\text{LaPO}_4$ [15], $\text{Ag}_3\text{PO}_4/\text{g-C}_3\text{N}_4$ [16,17], $\text{Ag}_3\text{PO}_4/\text{MoS}_2$ [18] were successfully synthesized and improved activity and stability of photocatalyst. The responsible mechanism of these heterostructures could be a direct band-band transfer [19] and Z-scheme mechanism [17,20] between Ag_3PO_4 and its coupled semiconductor. A direct band-band transfer could be defined that the photogenerated electron in the CB of coupled semiconductor is transferred into the CB of Ag_3PO_4 and the photogenerated holes in the valence band (VB) of Ag_3PO_4 is transferred into the VB of coupled semiconductor [17]. In this mechanism, the hole of coupled semiconductor oxidizes the pollutants and the electron in the CB of Ag_3PO_4 produced reactive oxygen species during photocatalytic reaction. The Z-scheme mechanism could be defined that the photogenerated electrons in the CB of Ag_3PO_4 and photogenerated

* Corresponding author.

E-mail address: uyi.sulaeman@yahoo.com (U. Sulaeman).

holes in the VB of coupled semiconductor combine directly [20] or through metallic particle contacted with both Ag_3PO_4 and coupled semiconductor [18,21,22]. This mechanism generates holes in the VB of Ag_3PO_4 and electron in the CB of coupled semiconductor [17].

The third strategy is the surface modification of Ag_3PO_4 by various electron or hole co-catalysts. This method can improve the photocatalytic performance via promoting the rapid transfer and separation of photogenerated charges. The Ag_3PO_4 surface could be modified by Co-Pi as hole cocatalyst that improved the photocatalytic activity [23]. The simultaneous loading of Ag nanoparticles and Fe(III) co-catalyst could improve the photocatalytic activity of Ag_3PO_4 [24]. This Ag nanoparticles can generate the surface plasmon resonance and improves the bandgap visible-light absorption of Ag_3PO_4 , resulting in the generation of more photogenerated charges. The surface of Ag_3PO_4 could also be modified by incorporating graphene to form $\text{Ag}_3\text{PO}_4/\text{graphene}$ composite [25,26]. This modification improved the surface area, absorption of organic dyes and separation of photogenerated electron-hole pairs [25]. Incorporating graphene on the Ag_3PO_4 also improved the morphology in which the Ag_3PO_4 dispersed uniformly on the graphene sheets surface [26].

Recently, the presence of native defects in Ag_3PO_4 catalyst has tremendously attracted the attention of researchers [27]. Ag_3PO_4 with oxygen vacancy could be generated by calcination method [28]. During calcination, metallic Ag nanoparticle are formed and deposited on the surface of Ag_3PO_4 . Oxygen vacancies have significant positive effect in improving the activity, whereas the metallic Ag nanoparticles have a very important effect in improving the stability. Chong et al. [29] reported that high temperature calcination of Ag_3PO_4 induced the oxygen vacancies. It is known that the enhanced photocatalytic activity of Ag_3PO_4 depends on crystallinity, oxygen vacancies and specific surface area. Unfortunately, the oxygen vacancy in Ag_3PO_4 has a relatively high formation energy compared to silver vacancy and silver interstitial because of the strong P-O bond that must be broken to remove an O atom [27]. Due to the strong P-O valence, PO_4^{3-} ions are difficult to form oxygen vacancies [30]. Therefore, generating the silver vacancy could be a promising approach to boost activity of Ag_3PO_4 . Yan et al. [31] successfully synthesized Ag_3PO_4 with formation of metallic Ag and high Ag vacancies using silver acetate as the precursor followed by calcination. The improved photocatalytic activity of this material was due to the synergistic effect of Ag vacancies and metallic Ag, which contributed to the efficient separation of photogenerated charge carriers. Ma et al. [30] suggested that defect states of Ag vacancies could act as capture traps for photoexcited holes and enhanced the separation of photogenerated electron-hole pairs.

Here, native defects of Ag vacancy in Ag_3PO_4 were generated using co-precipitation method under ethanol-aqueous solution. AgNO_3 dissolved in ethanol-aqueous solution with the ethanol contents of 0%, 25%, 50%, 75%, 90% and 100% was reacted to Na_2HPO_4 aqueous solution. The enhanced composition of ethanol in the synthesis of Ag_3PO_4 decreased the Ag/P atomic ratio in Ag_3PO_4 . These defects might facilitate the enhanced separation of photogenerated electron-hole which improved the photocatalytic activity.

2. Experimental

Silver vacancies of Ag_3PO_4 were prepared using co-precipitation method. Typically, 0.85 g of AgNO_3 was dissolved in 200 mL of ethanol-aqueous solution with ethanol contents of 0%, 25%, 50%, 75%, 90% and 100%. These samples were named as Et-0, Et-25, Et-50, Et-75, Et-90 and Et-100, respectively. AgNO_3 in ethanol-aqueous solution was slowly added (dropwise) by Na_2HPO_4 aqueous solution which was prepared by dissolving of 1.79 g of $\text{Na}_2\text{HPO}_4 \cdot 12\text{H}_2\text{O}$ in 50 mL of water. The precipitates in this reaction were separated

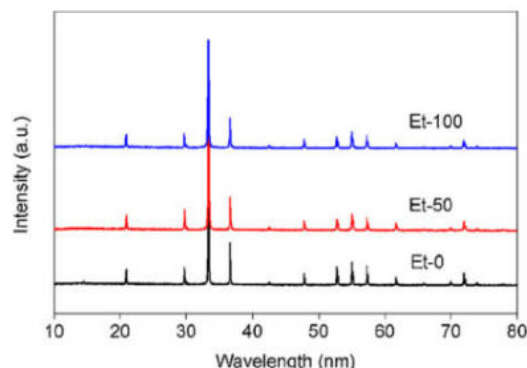


Fig. 1. XRD of Ag_3PO_4 synthesized using Na_2HPO_4 aqueous solution with AgNO_3 in ethanol (Et-100), 50% ethanol (Et-50) and without ethanol (Et-0).

by 14,000 rpm centrifugation and washed with distilled water and acetone three times, and subsequently dried in a vacuum oven at 60°C .

The Ag_3PO_4 samples were characterized by X-ray diffraction (XRD, Bruker AXS D2 Phaser), while the diffuse reflection spectra were obtained using a UV-vis NIR spectrometer (JASCO V-670). The specific surface areas were determined by BET measurements (NOVA 4200e). The morphologies of the powders were observed by an FE-SEM (Hitachi, S-4800). The X-ray photoelectron spectra were obtained using an X-ray photoelectron spectrometer (XPS, Perkin Elmer PHI 5600).

The photocatalytic activities were evaluated based on the rate of Rhodamine B decomposition after dispersing 0.1 g of photocatalyst to 100 mL of 10 mg/L Rhodamine B aqueous solution. The mixture was stirred at room temperature for 20 min (under dark condition) and the 2.5 W of LED blue light (OptiLED, SP-E27BL, 2.5 W) was used for irradiation. Four mL of sample solution was withdrawn every 10 min and centrifuged at 14,000 rpm to separate the catalyst. The concentration of Rhodamine B was measured using a spectrophotometer (JASCO V-670). The highest photocatalytic activity was also evaluated using phenol (colorless pollutant) decomposition under blue light irradiation with the higher power (Duralux, E-27, 3 W). The phenol concentration was determined using 4-aminoantipyrine method.

The mechanisms of photocatalysis were investigated using the scavengers of radical and holes in photocatalytic reaction (10 mg/L RhB, 100 mL solution, 0.1 g catalyst) under blue light irradiation (Duralux, E-27, 3 W). The benzoquinone (BQ), isopropyl alcohol (IPA) and ammonium oxalate (AO) were added into solution as scavenger of superoxide ion ($\text{O}_2^{\cdot-}$) radical, hydroxyl ($\cdot\text{OH}$) radical and holes, respectively [32]. The scavenger dosage was 1 mmol/L and the concentration of Rhodamine B was measured using a spectrophotometer.

3. Results and discussion

A yellow-crystalline Ag_3PO_4 catalyst was successfully synthesized by a simple method of co-precipitation using AgNO_3 and $\text{Na}_2\text{HPO}_4 \cdot 12\text{H}_2\text{O}$ as the starting materials. The AgNO_3 ethanol-aqueous solution with the ethanol concentrations of 0%, 25%, 50%, 75%, 90% and 100%, were successfully co-precipitated with Na_2HPO_4 aqueous solution. The XRD profiles shows that the structure body-centered cubic (JCPDS no.06-0505) with the space group of P4-3n is observed in Et-0, Et-50 and Et-100 (Fig. 1). No impurities were detected in all samples, indicating that they are single phase. There is no difference of lattice constants that

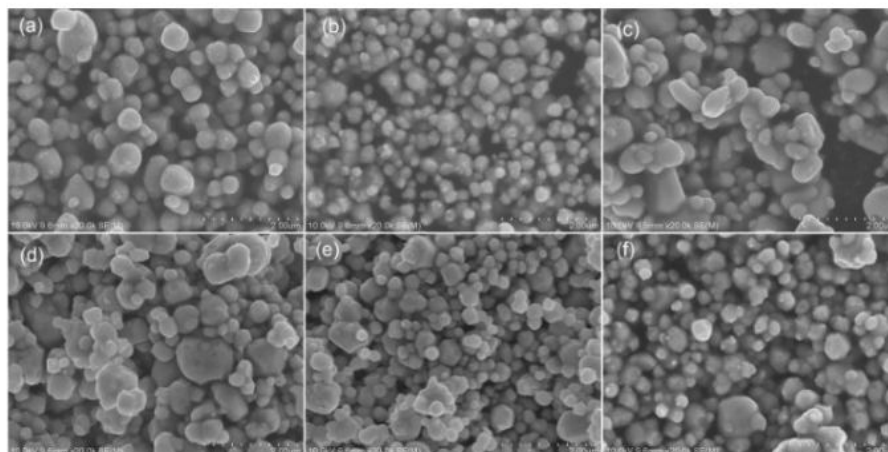


Fig. 2. SEM images of Ag_3PO_4 synthesized using Na_2HPO_4 aqueous solution and AgNO_3 in different compositions of ethanol-water: Et-0 (a), Et-25 (b), Et-50 (c), Et-75 (d), Et-90 (e) and Et-100 (f).

Table 1
Specific surface area, band gap energy and rate constant of Ag_3PO_4 synthesized under different compositions of ethanol-water solution.

Sample	S.S.A. (m^2/g)	Band gap energy (eV)	K_{app} (min^{-1})
Et-0	7.18	2.40	0.018
Et-25	8.34	2.37	0.051
Et-50	4.46	2.38	0.105
Et-75	7.67	2.37	0.095
Et-90	4.11	2.38	0.106
Et-100	9.12	2.40	0.069

could be observed in the samples. The lattice constants of 6.0148 Å, 6.0149 Å, 6.0149 Å could be calculated in the Et-0, Et-50 and Et-100, respectively. All structures were similar to those reported previously using H_3PO_4 in ethanol solution as the source of phosphate ion [8]. However, in the recent synthesis, there was no tetrahedral morphology that could be formed. The sphere and irregular shapes were clearly observed in all samples with the particle sizes of 200–600 nm as shown in Fig. 2(a–f). Specific surface areas of 4.46–9.12 m^2/g could be obtained and there is no significant difference of the specific surface area (Table 1). These indicated that the high photocatalytic activity did not depend on specific surface area or morphologies. Some other effects such as defect properties should be investigated to understand the reason of enhanced photocatalytic activity.

Fig. 3 shows the absorption spectra of Et-0, Et-50 and Et-100. It is clearly noted that the broad absorption above 500 nm increased in Et-50 and Et-100. It indicates that the ethanol treatment in the solution affects the optical properties of Ag_3PO_4 . The absorption of Ag_3PO_4 is very important to act as a visible-responsive photocatalyst. Some researchers found that the broad absorption in visible region might come from the defect sites of crystals as found in TiO_2 [33] and SrTiO_3 [34]. In this experiment, the broad absorption in visible region could be found in Ag_3PO_4 prepared by ethanol-water solution. The E_g and gap energy (E_g) of photocatalyst can be calculated using the following equation [35]: $\alpha h\nu = A(h\nu - E_g)^{n/2}$ where α , h and ν are the absorption coefficient, Planck constant, light frequency, respectively, while A is a constant and the value of n depends on whether the transition is direct ($n=1$) or indirect ($n=4$). The calculated band gap energies of all samples are similar as shown in Table 1. Therefore, the phenomenon of broad absorption in visible region might play a key role in photocatalytic activity

under visible light irradiation. This phenomenon is also discussed in detail in the section of XPS analysis.

Fig. 4 shows the photocatalytic decomposition of Rhodamine B (RhB) under blue light irradiation (LED 2.5 W). The apparent pseudo-first-order kinetics equation of $\ln(C_0/C) = K_{\text{app}}t$ was used to evaluate the rate of photocatalytic reaction, where K_{app} is the apparent pseudo-first-order rate constant (min^{-1}), C and C_0 are the RhB concentration at time t and zero, respectively [36,37]. The calculated values of K_{app} are summarized in Table 1. Based on these results, all samples synthesized with the ethanol-water solution showed higher activity. The highest activities were observed in Et-50 and Et-90. The photocatalytic activity could be improved to about 5.8 times higher than that of the Et-0. This activity was higher than the previous result of saddle-like Ag_3PO_4 which was about 3 times higher compared to its control [8]. This observation suggests that the activity of Ag_3PO_4 was significantly affected by the type of starting materials and composition of solution. In this experiment, the photocatalytic activities were significantly influenced by the properties of Ag_3PO_4 which was formed by varying the ethanol content in the Ag^+ solution and Na_2HPO_4 aqueous solution. The different properties might be attributed to different co-precipitation condition due to different polarity of the mixed

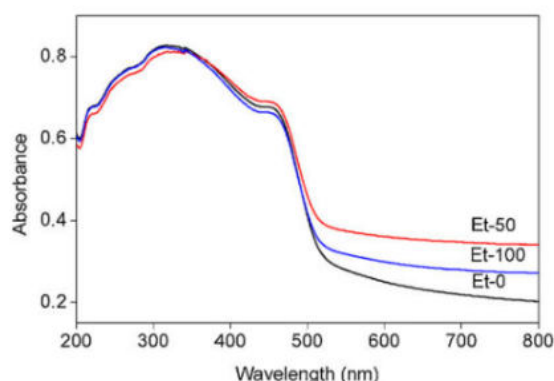


Fig. 3. DRS of Ag_3PO_4 synthesized using Na_2HPO_4 aqueous solution and AgNO_3 in ethanol (Et-100), 50% ethanol in ethanol-water solution (Et-50) and without ethanol (Et-0).

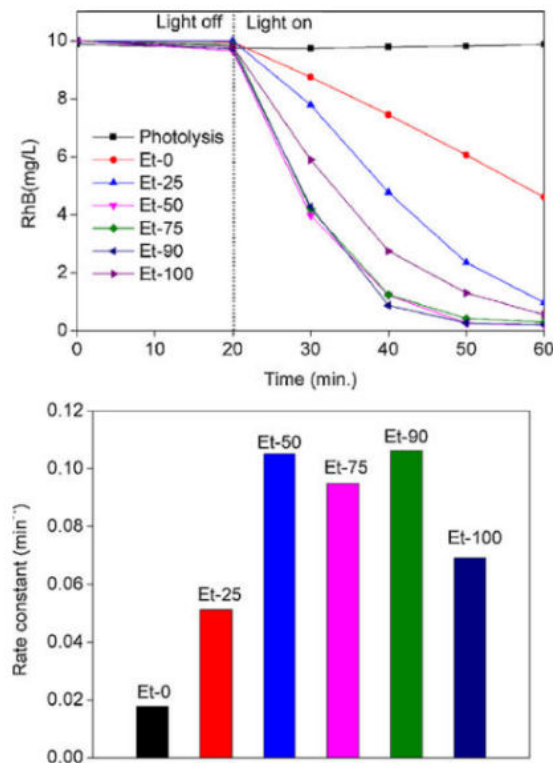


Fig. 4. Photocatalytic activities of Ag_3PO_4 synthesized using Na_2HPO_4 aqueous solution and AgNO_3 in different compositions of ethanol-water: Et-0, Et-25, Et-50, Et-75, Et-90 and Et-100 under blue light irradiation (LED 2.5W).

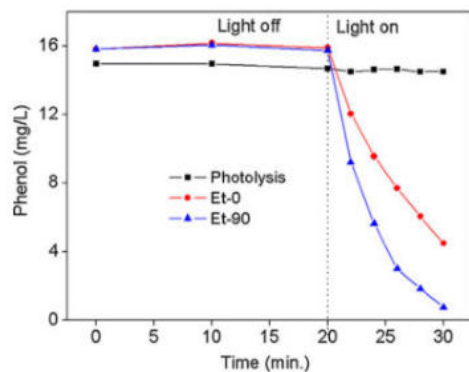


Fig. 5. Photocatalytic phenol degradation using Et-0 and Et-90 under blue light irradiation (LED 3 W).

solutions. The mixed solution would affect the migration of ions in the solution and influence the co-precipitation, which causes the defect sites trapped in the bulk or the surface of Ag_3PO_4 particles. These native defects might be a silver vacancy state which facilitates the enhanced separation of photogenerated electron-hole.

To ensure the effect of defect sites, the photocatalytic activity was also applied to decompose the phenol compound (the colorless pollutant) under blue light irradiation with the higher power of LED lamp (3 W) (Fig. 5). The highest photocatalytic activity of Et-90 was evaluated by phenol decomposition and the result was compared

Table 2

Peak energy and FWHM of Ag4d, P2p and O1s from the XPS analysis.

Sample	Element	Peak energy (eV)	FWHM (eV)
Et-0	Ag4d	4.99	2.90
	P2p	132.61	2.13
	O1s(O1)	530.52	1.62
Et-50	O1s(O2)	532.34	2.06
	Ag4d	5.00	2.80
	P2p	132.86	2.23
Et-100	O1s(O1)	530.60	1.55
	O1s(O2)	532.46	2.03
	Ag4d	4.81	2.77
	P2p	132.74	2.21
	O1s(O1)	530.52	1.53
	O1s(O2)	532.40	1.93

to Et-0. The rate constant of 0.286 min^{-1} could be observed in Et-90 which is significantly higher than that of Et-0 (0.124 min^{-1}) indicating that the photocatalyst is not only active for color pollutant degradation but also for colorless pollutant.

The XPS investigation was carried out to understand the properties of Et-0, Et-50 and Et-100 (Fig. 6 (a,b)). The peaks at 4.99 eV, 5.00 and 4.81 eV could be attributed to Ag4d of Et-0, Et-50 and Et-100 respectively. The peak energy of Ag4d of Et-50 is similar to that of Et-0, whereas the peak of Et-100 shifts to the lower binding energy by 0.18 eV. The peak energies of 132.61, 132.86 and 132.74 eV attributed to P^{5+} of Ag_3PO_4 are observed in Et-0, Et-50 and Et-100 respectively [38]. The peak energy of P2p is shifted by 0.25 eV to a higher energy for Et-50. Interestingly, the full width at half maximum (FWHM) of Ag4d decreases with the addition of ethanol whereas the FWHM of P2p increases with the addition of ethanol in synthesis of Ag_3PO_4 . The decreased FWHM of Ag4d and increased FWHM of P2p might be attributed to the silver vacancy formation. The details of peak energy and FWHM of Et-0, Et-50 and Et-100 are summarized in Table 2.

The changes of these states could be explained by theoretical aspect of Ag vacancy as described by Reunchan and Umezawa [27]. The Ag vacancy (V_{Ag}) formation did not require much energy because the Ag–O bonds are weak and can be easily broken, whereas oxygen vacancy (V_{O}) needs high energy due to the strong bonding of P–O. With the absence of Ag atom, the partially occupied states in the band gap could be created. These were mostly derived from the d orbitals of a neighboring Ag atom. These states could accept an additional electron to form a single acceptor of Ag vacancy (V_{Ag}). As the V_{Ag} is an acceptor, the negative charge state (V_{Ag}^-) is more easily formed when Fermi energy (ϵ_F) increases.

The decreased FWHM of Ag4d might be the consequence of shorter distance of the two Ag atoms due to the V_{Ag} . Theoretically [27], the distance of the two Ag atoms across the V_{Ag} is shorter than the equilibrium distance of the corresponding two Ag atoms in the perfect crystal. The strong attractive interaction between the V_{Ag} and the neighboring Ag atoms might lead to a high V_{Ag} mobility. The low energy migration barrier of V_{Ag} suggests that the V_{Ag} probably migrates along the path which involves the displacement of the nearest-neighboring Ag atom. Therefore, the silver vacancies could not be the isolated defects. They could bind with other defects or impurities, diffuse out of the bulk region, or possibly migrate and become trapped on the surface of the Ag_3PO_4 particles.

The atomic ratio of Ag/P significantly decreases by increasing the ethanol content indicating that the silver vacancy could be easily created (Table 3). Theoretically [27], the main native defects of Ag_3PO_4 could be a silver vacancy (V_{Ag}), oxygen vacancy (V_{O}), silver interstitial (Ag_i), oxygen interstitial (O_i), and interstitial hydrogen (H_i). Among these defects, silver vacancy is easier created in Ag_3PO_4 due to low energy of formation. Previous work, the defects could be designed by non-stoichiometric synthesis of photocatalyst [39]. Here, the different polarity of the mixed solutions might also affect

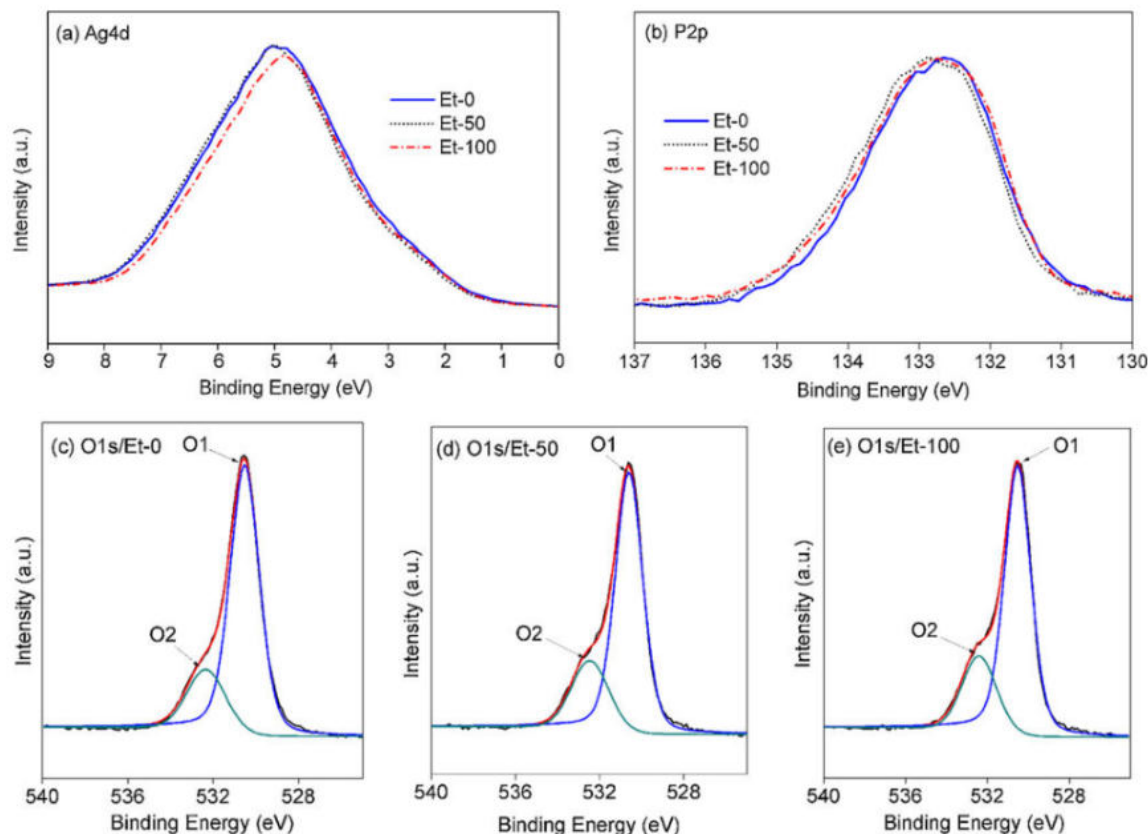


Fig. 6. XPS profiles of Ag_3PO_4 for Et-0, Et-50 and Et-100: the Ag4d (a), P2p (b) and O1s with the deconvolution of Et-0 (c), Et-50 (d) and Et-100 (e).

Table 3

Atomic ratios of Ag/P and O/Ag in the samples of Et-0, Et-50 and Et-100.

Sample	Atomic Ratio	
	Ag/P	O/Ag
Et-0	2.66	1.39
Et-50	2.57	1.52
Et-100	2.41	1.55

the atomic ratio of Ag_3PO_4 . The decrease of Ag/P atomic ratio, the decrement of the Ag4d FWHM and increment of P2p FWHM of Ag_3PO_4 indicate that the silver vacancies were formed.

The atomic ratio of O/Ag in Ag_3PO_4 increases by elevating the ethanol content of mixed solution (Table 3). To understand the type of oxygen in Ag_3PO_4 , the deconvolution of O1s peak should be created using the Lorentzian Gaussian fitting. There are two types of peaks (O1 and O2) were observed as shown in Fig. 6 (c–e). The O1 peak at 530.52 eV is related to O–Ag bonding whereas the O2 peak (shoulder peak) at 532.34 eV could be assigned to hydroxyl groups [29,40]. The O2 peak of hydroxyl groups might be attributed to the interaction of H_2O on the Ag_3PO_4 surface. From the deconvolution, the O2/O1 area ratio of 0.25, 0.29 and 0.32 could be calculated in Et-0, Et-50 and Et-100 respectively, indicating that the samples with the ethanol treatment might have higher amount of hydroxyl groups on the surface. The Ag vacancy created in Et-50 and Et-100 might enhance the interaction of PO_4^{3-} and H_2O in the surface. These can facilitate the formation of hydroxyl radical under visible light irradiation. The inductive effect of PO_4^{3-} could also enhance

the electron and holes separation, which plays an important role in photocatalysis [41].

Mechanisms of photocatalytic were investigated by adding the scavengers of radicals and holes to photocatalytic reaction [32]. The benzoquinone (BQ), isopropyl alcohol (IPA) and ammonium oxalate (AO) were added into the reaction solution as scavenger of superoxide ion ($\text{O}_2^{\cdot-}$) radicals, hydroxyl ($\cdot\text{OH}$) radicals and holes, respectively. The effect of these scavengers to photocatalytic reaction can be seen in Fig. 7. The BQ addition could significantly suppress the photocatalytic activity in both Et-0 and Et-50, indicating that their mechanisms involved the superoxide ion radicals. The addition of IPA suppress the photocatalytic activity of Et-50, suggesting that the mechanism involved the hydroxyl radicals which might be generated by the defect sites of Ag_3PO_4 surface, whereas the photocatalytic activity in Et-0 could not be significantly suppressed by adding IPA, indicating that the mechanism might not involve the hydroxyl radical. Generating hydroxyl radical in Et-50 correspond with the XPS analysis that showing the higher ratio of O2/O1 due to higher amount of hydroxyl group adsorption in the surface of Ag_3PO_4 . The PO_4^{3-} on the surface of Ag_3PO_4 might play as the strong bonding ability with H_2O that can promote hydroxyl radical formation. The addition of AO to Et-0 and Et-50 suppressed their photocatalytic activity, indicating both of them involved the holes mechanism. The higher suppression was found in Et-50, suggesting that the holes were highly involved in the mechanism of photocatalytic. The Ag vacancy sites in the band gap of Ag_3PO_4 will act as capture traps for photoexcited holes, which subsequently enhances the separation of electron-hole pairs resulting in improvement in

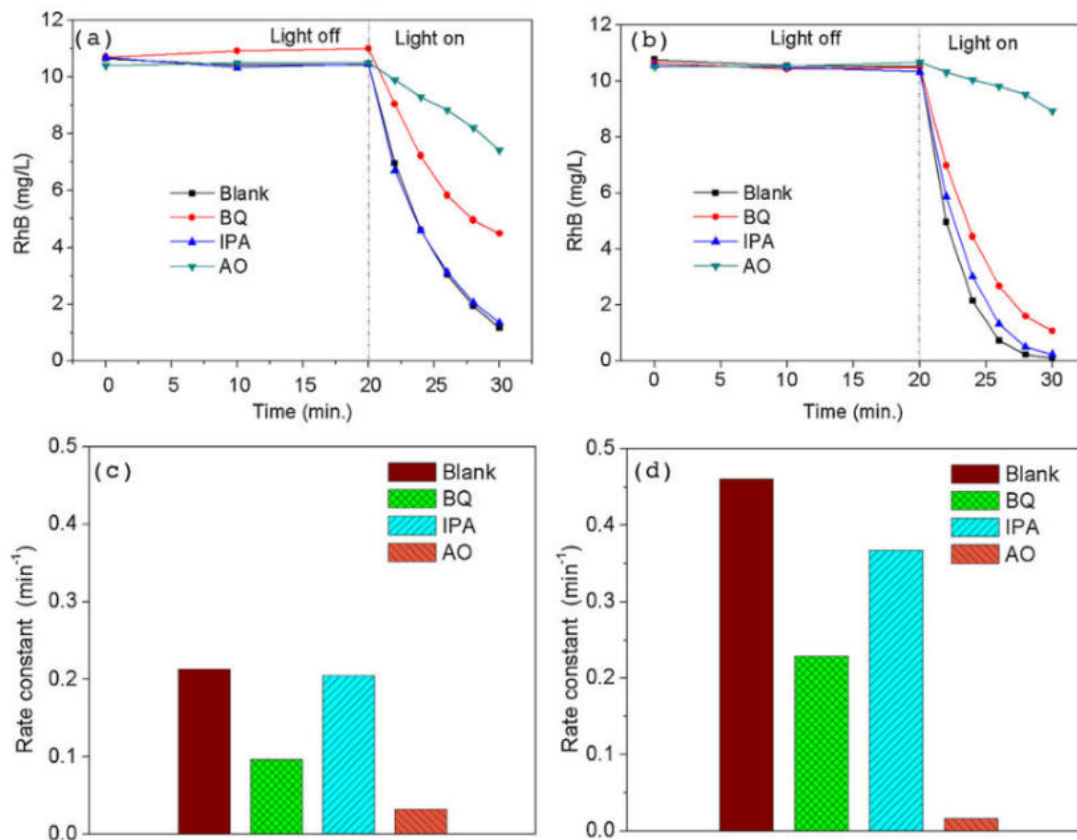


Fig. 7. The effect of benzoquinone (BQ), isopropyl alcohol (IPA) and ammonium oxalate (AO) on the photocatalytic reaction in Et-0 (a), Et-50(b) and the rate constant in Et-0 (c), Et-50(d).

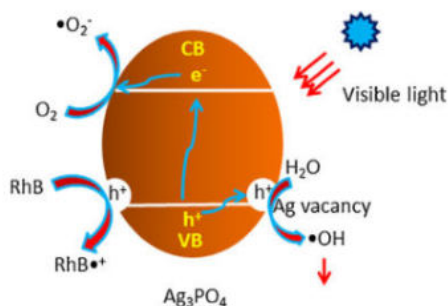


Fig. 8. The proposed mechanism of photocatalytic reaction in the surface of defect Ag_3PO_4 .

photocatalytic activity. The holes accumulated at the valence band of Ag_3PO_4 might directly oxidize RhB to produce RhB $^{\cdot+}$ radicals, and the excited electron at the conduction band of Ag_3PO_4 transfer to adsorbed oxygen to form $\text{O}_2^{\cdot-}$. The mechanism of photocatalytic reaction was proposed in Fig. 8

4. Conclusions

The Ag_3PO_4 photocatalyst with native defects were successfully synthesized through co-precipitation method using AgNO_3

ethanol-aqueous solution and Na_3PO_4 aqueous solution. Elevated ethanol concentration evidently decreased the Ag/P atomic ratio of Ag_3PO_4 . The broad absorption in visible region of DRS, the decrement of the Ag4d FWHM and increment of P2p FWHM might be caused by a silver vacancy formation on the surface of Ag_3PO_4 . The photocatalytic activity of Ag_3PO_4 with silver vacancy increases to about 5.8 times higher than that of the pristine Ag_3PO_4 . The defect states of Ag vacancies could act as capture traps for photoexcited holes, which subsequently enhances the separation of electron-hole pairs, leading to the enhancement of photocatalytic activity.

Acknowledgments

This research was financially supported by Directorate of Research and Community Services, Directorate General of Development and Research Enhancement, Ministry of Research, Technology and Higher Education of the Republic of Indonesia in the Scheme of Competency Grant, Contract Number: 068/SP2H/LT/DRPM/IV/2017.

References

- [1] D.J. Martin, N. Umezawa, X. Chen, J. Ye, J. Tang, *Energy Environ. Sci.* 6 (2013) 3380–3386.
- [2] Y. Bi, S. Ouyang, N. Umezawa, J. Cao, J. Ye, *J. Am. Chem. Soc.* 133 (2011) 6490–6492.
- [3] H. Wang, L. He, L. Wang, P. Hu, L. Guo, X. Han, J. Li, *CrystEngComm* 14 (2012) 8342–8344.

- [4] B. Zheng, X. Wang, C. Liu, K. Tan, Z. Xie, L. Zheng, *J. Mater. Chem. A* 1 (2013) 12635–12640.
- [5] H. Hu, Z. Jiao, H. Yu, G. Lu, J. Ye, Y. Bi, *J. Mater. Chem. A* 1 (2013) 2387–2390.
- [6] J. Wang, F. Teng, M. Chen, J. Xu, Y. Song, X. Zhou, *CrystEngComm* 15 (2013) 39–42.
- [7] P.W. Menezes, A. Indra, M. Schwarze, F. Schuster, M. Driess, *ChemPlusChem* 81 (2016) 1–8.
- [8] U. Sulaeman, F. Febiyanto, S. Yin, T. Sato, *Catal. Commun.* 85 (2016) 22–25.
- [9] L. Yang, W. Duan, H. Jiang, S. Luo, Y. Luo, *Mater. Res. Bull.* 70 (2015) 129–136.
- [10] P.S. Saud, B. Pant, A.P. Twari, Z.K. Ghouri, M. Park, H.-Y. Kim, *J. Colloid Interface Sci.* 465 (2016) 225–232.
- [11] C. Liu, X. Zhang, Q. Zhang, G. Meng, H. Zhao, J. Wu, Z. Liu, *J. Porous Mater.* 24 (2017) 179–187.
- [12] B. Liu, Y. Xue, J. Zhang, B. Han, J. Zhang, X. Suo, L. Mu, H. Shi, *Environ. Sci. Nano* 4 (2017) 255–264.
- [13] J. Guo, S. Ouyang, P. Li, Y. Zhang, T. Kako, J. Ye, *Appl. Catal. B Environ.* 134–135 (2013) 286–292.
- [14] C. Tang, E. Liu, J. Wan, X. Hu, J. Fan, *Appl. Catal. B Environ.* 181 (2016) 707–715.
- [15] F. Li, Z. Li, Y. Cai, M. Zhang, Y. Shen, X. Wang, M. Wu, Y. Li, C. Chen, X. He, *Mater. Lett.* 188 (2017) 343–346.
- [16] P. He, L. Song, S. Zhang, X. Wu, Q. Wei, *Mater. Res. Bull.* 51 (2014) 432–437.
- [17] L. Zhou, W. Zhang, L. Chen, H. Deng, *J. Colloid Interface Sci.* 487 (2017) 410–417.
- [18] C. Zhua, L. Zhang, B. Jiang, J. Zheng, P. Hu, S. Li, M. Wu, W. Wu, *Appl. Surf. Sci.* 377 (2016) 99–108.
- [19] N.N. Wang, Y. Zhou, C.H. Chen, L.Y. Cheng, H.M. Ding, *Catal. Commun.* 73 (2016) 74–79.
- [20] S. Meng, X. Ning, T. Zhang, S. Chen, X. Fu, *Phys. Chem. Chem. Phys.* 17 (2015) 11577–11585.
- [21] Y.F. Wang, J.X. Liu, Y.W. Wang, C.M. Fan, G.Y. Ding, *Mater. Sci. Semicond. Process.* 25 (2014) 330–336.
- [22] J.X. Liu, Y.F. Wang, Y.W. Wang, C.M. Fan, *Acta Phys.-Chim. Sin.* 30 (2014) 729–737.
- [23] P. Wang, S. Xu, Y. Xia, X. Wang, H. Yu, J. Yub, *Phys. Chem. Chem. Phys.* 19 (2017) 10309–10316.
- [24] H. Yu, G. Cao, F. Chen, X. Wang, J. Yu, M. Lei, *Appl. Catal. B Environ.* 160–161 (2014) 658–665.
- [25] X. Yang, H. Cui, Y. Li, J. Qin, R. Zhang, H. Tang, *ACS Catal.* 3 (2013) 363–369.
- [26] L. Xu, Y. Wang, J. Liu, S. Han, Z. Pan, L. Gan, *J. Photochem. Photobiol. A Chem.* 340 (2017) 70–79.
- [27] P. Reunchan, N. Umezawa, *Phys. Rev. B* 87 (2013) 245205.
- [28] P. Dong, G. Hou, C. Liu, X. Zhang, H. Tian, F. Xu, X. Xi, R. Shao, *Materials* 9 (2016) 968.
- [29] R. Chong, X. Cheng, B. Wang, D. Li, Z. Chang, L. Zhang, *Int. J. Hydrogen Energy* 41 (2016) 2575–2582.
- [30] X. Ma, B. Lu, D. Li, R. Shi, C. Pan, Y. Zhu, *J. Phys. Chem. C* 115 (2011) 4680–4687.
- [31] T. Yan, W. Guan, J. Tian, P. Wang, W. Li, J. You, B. Huang, *J. Alloy Compd.* 680 (2016) 436–445.
- [32] W. Liu, M. Wang, C. Xu, S. Chen, X. Fu, *Mater. Res. Bull.* 48 (2013) 106–113.
- [33] I. Nakamura, N. Negishi, S. Kutsuna, T. Ihara, S. Sugihara, K. Takeuchi, *J. Mol. Catal. A: Chem.* 161 (2000) 205–212.
- [34] H. Tan, Z. Zhao, W. Zhu, E.N. Coker, B. Li, M. Zheng, W. Yu, H. Fan, Z. Sun, *ACS Appl. Mater. Interfaces* 6 (2014) 19184–19190.
- [35] M.A. Butler, *J. Appl. Phys.* 48 (1977) 1914–1920.
- [36] Y. Li, X. Li, J. Li, J. Yin, *Water Res.* 40 (2006) 1119–1126.
- [37] U. Sulaeman, X. Wu, B. Liu, S. Yin, T. Sato, *Appl. Surf. Sci.* 356 (2015) 226–231.
- [38] R. Zheng, L. Lin, J. Xie, Y. Zhu, Y. Xie, *J. Phys. Chem. C* 112 (2008) 15502–15509.
- [39] U. Sulaeman, S. Yin, T. Sato, *Appl. Phys. Lett.* 97 (2010) 103102.
- [40] W. Teng, X. Li, Q. Zhao, G. Chen, *J. Mater. Chem. A* 1 (2013) 9060–9068.
- [41] C. Pan, Y. Zhu, *Environ. Sci. Technol.* 44 (2010) 5570–5574.

Native defects in silver orthophosphate and their effects on photocatalytic activity under visible light irradiation

ORIGINALITY REPORT

11%

SIMILARITY INDEX

7%

INTERNET SOURCES

8%

PUBLICATIONS

2%

STUDENT PAPERS

PRIMARY SOURCES

- | | | |
|---|--|----|
| 1 | jcc.undip.ac.id
Internet Source | 3% |
| 2 | epubs.surrey.ac.uk
Internet Source | 1% |
| 3 | Ma, Xinguo, Bin Lu, Di Li, Rui Shi, Chenshi Pan, and Yongfa Zhu. "Origin of Photocatalytic Activation of Silver Orthophosphate from First-Principles", The Journal of Physical Chemistry C, 2011.
Publication | 1% |
| 4 | Li Zhou, Wei Zhang, Ling Chen, Huiping Deng. "Z-scheme mechanism of photogenerated carriers for hybrid photocatalyst Ag ₃ PO ₄ /g-C ₃ N ₄ in degradation of sulfamethoxazole", Journal of Colloid and Interface Science, 2017
Publication | 1% |
| 5 | Sugang Meng, Xiaofeng Ning, Tao Zhang, Shi-Fu Chen, Xianliang Fu. "What is the transfer mechanism of photogenerated carriers for the nanocomposite photocatalyst Ag PO /g-C | 1% |

N , band–band transfer or a direct Z-scheme?

", Physical Chemistry Chemical Physics, 2015

Publication

6

ejournal2.undip.ac.id

Internet Source

1 %

7

Hongyan Hu, Zhengbo Jiao, Hongchao Yu, Gongxuan Lu, Jinhua Ye, Yingpu Bi. "Facile synthesis of tetrahedral Ag₃PO₄ submicro-crystals with enhanced photocatalytic properties", Journal of Materials Chemistry A, 2013

Publication

1 %

8

Yan, Tingjiang, Wenfei Guan, Jun Tian, Peng Wang, Wenjuan Li, Jinmao You, and Baibiao Huang. "Improving the photocatalytic performance of silver phosphate by thermal annealing: Influence of acetate species", Journal of Alloys and Compounds, 2016.

Publication

1 %

9

Fang, Shun, Kangle Lv, Qin Li, Hengpeng Ye, Dongyun Du, and Mei Li. "Effect of acid on the photocatalytic degradation of rhodamine B over g-C₃N₄", Applied Surface Science, 2015.

Publication

1 %

10

Chong, Ruifeng, Xiaoxue Cheng, Baoyun Wang, Deliang Li, Zhixian Chang, and Ling Zhang. "Enhanced photocatalytic activity of Ag₃PO₄ for oxygen evolution and Methylene

1 %

blue degeneration: Effect of calcination temperature", International Journal of Hydrogen Energy, 2016.

Publication

11

Submitted to School of Engineering, The University of Tokyo

Student Paper

1 %

12

Uyi Sulaeman, Richo Dwi Permadi, Dian Riana Ningsih, Hartiwi Diastuti, Anung Riapanitra, Shu Yin. "The surface modification of Ag₃PO₄ using anionic platinum complexes for enhanced visible-light photocatalytic activity", Materials Letters, 2020

Publication

1 %

Exclude quotes Off
Exclude bibliography On

Exclude matches < 1%